NONLINEAR VARIABLE LAG SMOOTHER

James R Wright* **James Woodburn†**

Abstract

Our new forward running Varible Lag Smoother (VLS) solves nonlinear multidimensional estimation problems, provides results in near-real-time, combines filter and smoothing calculations with one user specified operation, and does *not* require calculation of a state-sized covariance matrix *inverse*. Our use of a variable smoothing lag enables optimal solutions of existing orbit determination problems.

INTRODUCTION

We are working on solutions to the estimation problems associated with near-real-time orbit determination that are defined in sections *General Application*, *Impulsive Maneuvers*, *Global Atmospheric Density Estimation*, and *GPS Carrier-phase as Range*. See the section *Desired Properties* for the estimator we seek. See the section *Properties Available* for choices. So we are currently developing an estimator that combines a real-time extended Kalman filter (EKF) with a fixed epoch smoother[1] (FES), where the fixed epoch lags EKF measurement time-tags with variable time lag. Thus the name *variable lag smoother* (VLS).

We have implemented two forms of the FES, the Frazer form (FES/F), and the Carlton-Rauch form (FES/CR). FES/F is free of state-sized matrix inverse calculation, but FES/CR requires the calculation of a state-sized covariance matrix inverse for each FES/CR execution.

Orbit Determination Tool Kit (ODTK)[2] previously and currently provides a forward-running EKF, followed by a backward-running fixed-interval smoother (FIS). Two separate user operations are required to run the EKF-FIS filter-smoother. Fortunately the EKF runs in real-time and does *not* require calculation of a state-sized covariance matrix inverse. Unfortunately the FIS *does* require calculation of a state-sized covariance matrix inverse, and is not applicable to near-real-time operations.

Our new forward running VLS does *not* require calculation of a state-sized covariance matrix inverse for FES/F, provides results in near-real-time, and combines filter and smoothing calculations with one user selected operation.

GENERAL APPLICATION

Figure 1 illustrates a general application of our VLS with fixed epochs on a uniform time grid. A smoother window is anchored to each fixed epoch. Smoother window definition logic is selected by the user at run-time. The most simple user option is to select fixed constant window length for each smoothing window. Or the user may select time-varying criteria that require satisfaction of accuracy thresholds by time-varying covariance matrix elements, together with maxima of smoother window length. Smoother windows may be overlapping as in Figure 1, or they may be non-overlapping, and possibly on a non-uniform time grid, as in Figure 2.

*ODTK Architect, Analytical Graphics, Inc., 220 Valley Creek Blvd, Exton, PA, 19341

†Chief Orbital Scientist, Analytical Graphics, Inc.

[1] Our *fixed epoch* is the *fixed point* referred to for the fixed point smoother[6].

[2] Orbit Determination Tool Kit was developed, and is offered, by Analytical Graphics, Inc.

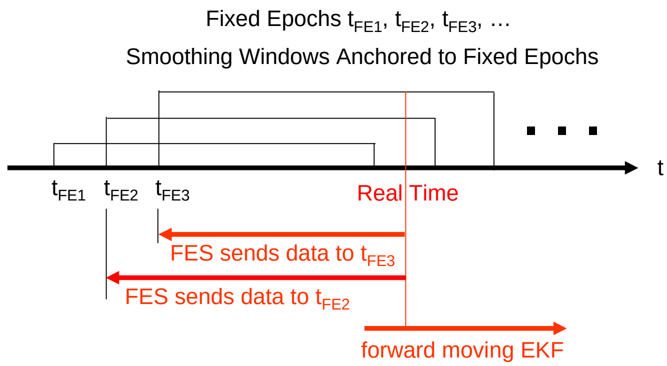

Figure 1: Variable Lag Smoother with EKF and FES

The EKF moves on a time grid dictated by measurement time-tags, generally non-uniform. When the EKF reaches a fixed epoch, a new FES is created. The FES estimate is initialized by the EKF estimate at the fixed epoch after all measurements have been processes by the EKF at the fixed epoch. As the EKF epoch moves forward, information derived from the EKF at each measurement time-tag is sent backwards to the fixed epoch by the FES while the EKF epoch is in the smoother window. The FES is invoked only for EKF measurement updates. The FES is not invoked for EKF time updates, unlike FIS operation. When the EKF epoch exits the smoother window the FES is destroyed, and associated smoother results are recorded. The lag of fixed epoch relative to the EKF epoch increases throughout passage of the smoother window by the EKF due to forward motion of the EKF epoch.

When a VLS computer run would be terminated with the EKF epoch inside of a smoothing window, the user will have an option to accept results of the VLS with partial completion of the last smoothing window, or to save results into an EKF restart file just prior to entry of the EKF epoch into the last smoothing window.

ODTK LEO Simulation

Results

Figures 5, 6, 7, and 8 present[3] ODTK intrack position results from processing simulated two-way range measurements from eight AFSCN ground stations and a LEO spacecraft with transponder. Figure 5 presents estimation errors for VLS (using FES/F), and demonstrates consistency of the VLS covariance matrix function with estimation errors. Figure 6 demonstrates accuracy equivalence of the VLS with the FIS.

Figure 7 contrasts performance of the VLS FES with the VLS EKF. The outside covariance error envelope is defined by the EKF, and the inside covariance error envelope is defined by the FES. The forward running EKF creates a new FES at each fixed epoch according to user input at run-time. Here the fixed epochs are generated with one minute granularity. A smoother window follows each fixed epoch according to user selection at run-time. Here each smoother window is 300 minutes in length. The FES sends EKF information backwards to the fixed epoch while the forward running EKF remains in the smoother window. Each FES is destroyed when the EKF exists the smoother window. Thus the FES has a maximum lag from real-time of 300 minutes for this example.

Accuracy improvement due to 300 minute smoother windows over 100 minute smoother windows is presented with Figure 8. The new VLS enables trading maximum lag time for accuracy performance.

[3] These figures are oversized to enable reading graphical details, and were placed after the list of references.

Input Data

Initial LEO orbit element values and initial orbit error root-variance values for the simulation are presented in Table 1.

Orbit Element	Value	Root Variance	Value
semi-major axis (er)	1.08	radial pos (m)	100.0
eccentricity	0.04	intrack pos (m)	1000.0
true arg latitude (deg)	120.0	crosstrack pos (m)	50.0
inclination (deg)	100.0	radial vel (m/s)	1.0
node (deg)	60.0	intrack vel (m/s)	0.1
arg of perigee (deg)	30.0	crosstrack vel (m/s)	0.5

Table 1: Simulated LEO Initial Conditions

The spacecraft was simulated as a sphere with mass $M = 1000$ kg, ballistic coefficient $C_D = 2.0$, and reference cross-sectional area $A = 20.0$ m^2. The root-variance on relative ballistic coefficient error $\sigma_{\Delta B/B} = 0.1$, with exponential half-life $\tau_{\Delta B/B} = 1$ year. For atmospheric density we used the CIRA 1972 model, and specified an error exponential half-life $\tau_{\Delta\rho/\rho} = 180$ minutes. The root-variance on solar pressure $\sigma_{CP} = 0.2$, with exponential half-life $\tau_{CP} = 21$ days. White-noise root-variance on the two-way range measurements was $\sigma_R = 5$ meters. The six components of position and velocity, one atmospheric density parameter, one ballistic coefficient parameter, and one solar pressure parameter were estimated.

IMPULSIVE MANEUVERS

Consider a single spacecraft that performs impulsive[4] maneuvers, and consider the sequential estimation of the state from tracking measurements. The state includes the six components of position and velocity, force model parameters, and time-varying measurement biases.

ODTK does successfully estimate velocity change due to an impulsive maneuver using the FIS, but this is an off-line operation, relative to the ODTK EKF. The FIS estimation runs backward with time.

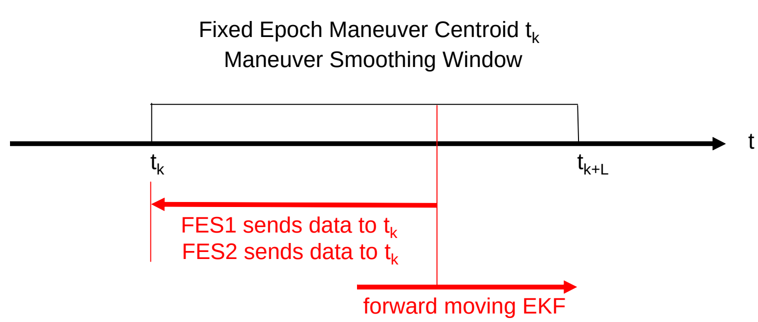

Figure 2: Estimation of Velocity at Fixed Epochs with EKF and FES

Our new VLS method eliminates the off-line FIS, uses a forward running EKF, and uses two FES smoothers that send EKF estimate information backwards to a fixed epoch. The fixed epoch is defined by an impulsive maneuver time centroid, say t_k as illustrated in Figure 2.

[4] Impulsive maneuvers are used to model thrust intervals that are short as compared to orbit period.

Let t_k denote the time centroid of an impulsive spacecraft maneuver. Let $\hat{X}_{k|i}^{(-)}$ and $P_{k|i}^{(-)}$ denote the state estimate and covariance derived by the EKF from processing the last measurement y_i with time-tag $t_i \leq t_k$. The estimate $\hat{X}_{k|i}^{(-)}$ does *not* include addition of the velocity change at t_k, and its associated covariance matrix $P_{k|i}^{(-)}$ does not include the addition of EKF maneuver process noise covariance at t_k. The EKF state estimate $\hat{X}_{k|i}^{(-)}$ and covariance matrix $P_{k|i}^{(-)}$ are used to initialize FES1 at time t_k.

Let $\hat{X}_{k|i}^{(+)}$ and $P_{k|i}^{(+)}$ denote the state estimate and covariance derived after application of velocity change to $\hat{X}_{k|i}^{(-)}$, and after addition of maneuver process noise covariance to $P_{k|i}^{(-)}$. The state estimate $\hat{X}_{k|i}^{(+)}$ and covariance matrix $P_{k|i}^{(+)}$ are used to initialize FES2 at time t_k. A smoothing window $\{t_k, t_{k+L}\}$ is selected by the user, explicitly or implicitly. Now we process measurements y_j, $j = k+1, k+2, \ldots, k+L$ by the EKF, and operate both FES1 and FES2 on the EKF output across the smoothing window $\{t_k, t_{k+L}\}$. The VLS with two FES smoothers produces smoothed estimates $\hat{X}_{k|k+L}^{(-)}$ and $\hat{X}_{k|k+L}^{(+)}$, and their covariance matrices $P_{k|k+L}^{(-)}$ and $P_{k|k+L}^{(+)}$. The desired estimate of velocity change is found in the velocity components of the difference $\hat{X}_{k|k+L}^{(+)} - \hat{X}_{k|k+L}^{(-)}$.

Conjectures

- The VLS is applicable to estimation of impulsive maneuvers of hostile spacecraft, where the time centroids are initially unknown
- The VLS can be extended to estimate finite (non-impulsive) maneuvers of friendly spacecraft and hostile spacecraft from tracking data

Development Status

The VLS has been validated with simulations for impulsive maneuvers of friendly spacecraft.

GLOBAL ATMOSPHERIC DENSITY ESTIMATION

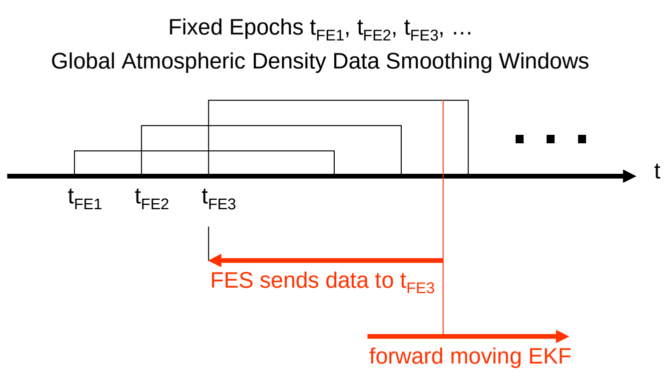

Figure 3: Estimation of Orbits and Global Atmospheric Density

Consider the simultaneous orbit determination of an ensemble of LEO spacecraft, together with estimation of atmospheric density and ballistic coefficient for each spacecraft, the estimation of global parameters of atmospheric density that drive a physically connected time-varying model, and the estimation of appropriate time-varying measurement biases. Tracking data are received on all LEO spacecraft and are processed by the EKF as they are received. At run-time the user selects smoother windows that are anchored to fixed epochs $t_{\rm FE1}$, $t_{\rm FE2}$, $t_{\rm FE3}$, ... When the time-varying EKF epoch

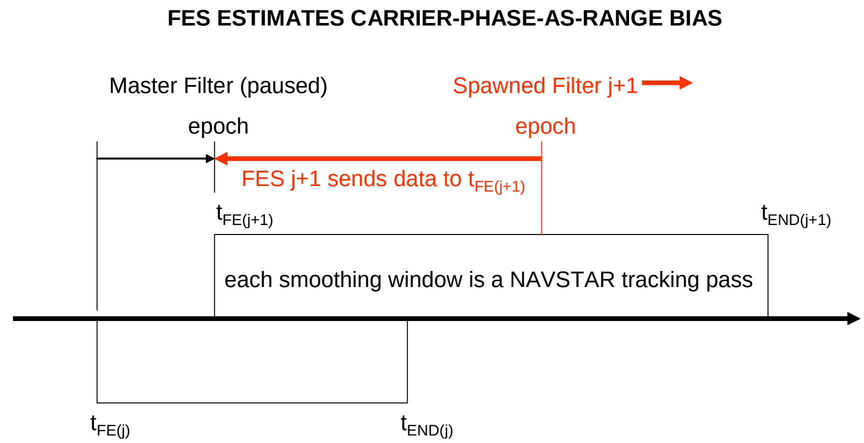

Figure 4: VLS for NAVSTAR Orbits, Clocks, and Carrier-Phase Range Biases

t_{filter} reaches $t_{\text{FE}n}$, for $n = 1, 2, 3, \ldots$, an FES is initialized there and the FES estimate of global atmospheric density is improved at $t_{\text{FE}n}$ until the EKF exits the $t_{\text{FE}n}$ smoothing window. The time-varying global atmospheric density model can be propagated forward from the last fixed epoch to provide optimal predictions of global atmospheric density with estimation error covariance.

Development Status

Figures 9 and 10 were presented[19] in Maui in 2004. Figure 9 presents an overlay of simulated and FIS smoothed atmospheric density ratios $\Delta\rho/\rho$ for 8000 minutes. Figure 10 presents an overlay of simulated and EKF filtered atmospheric density ratios $\Delta\rho/\rho$ for the same 8000 minutes. The effect of a smoothing lag for atmospheric density estimation of a single spacecraft was thereby demonstrated.

GPS CARRIER-PHASE AS RANGE

Larson[2][3][5] and Levine have demonstrated the use of GPS carrier phase measurements for the most accurate method of time-transfer. We are indebted to Tom Parker[10][4] for bringing this work to our attention. Larson and Levine used an iterated least squares technique with the least squares epoch fixed at the initial time for each NAVSTAR carrier phase tracking interval.

The estimation of carrier phase range bias from ground station carrier phase measurements over phase count intervals of several hours, with the simultaneous processing of ground station pseudo-range measurements, enables the most accurate method for GPS time transfer. But currently there does not exist a technique to apply this representation of GPS Doppler carrier phase measurements to *near-real-time* operations. Here we propose a method to realize GPS time transfer with GPS carrier phase measurements in *near-real-time* using our VLS with an FES for each fixed epoch.

Consider a GPS NAVSTAR constellation of N spacecraft, where we estimate n state parameters for each NAVSTAR spacecraft. Figure 4 depicts a forward running EKF Master Filter (MF) with Nn state elements, two fixed epochs with two smoothing windows, a forward running EKF Spawned Filter (SF) with $n+1$ state elements for each smoothing window, and an FES with $n+1$ state elements for each fixed-epoch associated with each forward running SF. The $Nn \times 1$ column matrix state of the MF contains all NAVSTAR orbits, solar pressure parameters, and clock parameters. Each SF state and each FES state is an $(n + 1) \times 1$ matrix with the same structure. The $n \times 1$ substate matrix of each $(n + 1) \times 1$ matrix is also a substate of the MF state. Each SF state and each FES state contains an element for a constant carrier-phase-as-range bias, not contained in the MF state. State estimate and covariance for each SF and each FES are initialized at a fixed-epoch defined by the first carrier phase measurement for each NAVSTAR on a particular tracking data pass. The MF is paused at the fixed-epoch while the SF and FES operate across the smoothing window. The SF and FES exist for duration of the smoothing window defined by tracking data pass time interval. The $(n+1) \times 1$ matrix FES state is transformed to an $n \times 1$ matrix MF pseudo-measurement that is processed by the MF after the SF reaches the end of smoothing window. The SF and FES are destroyed at the end of each smoothing window. The MF continues, and survives indefinitely.

Potential Applications

Application 1

VLS could be used to perform near-real-time GPS time transfer, derived from a combination GPS pseudo-range measurements and GPS carrier-phase measurements.

Application 2

VLS could be used to optimally and simultaneously estimate GPS NAVSTAR orbits, clocks, and carrier-phase range biases at fixed epochs from a combination GPS pseudo-range measurements and GPS carrier-phase measurements. This VLS is applicable to the US Air Force GPS real-time operations. The MF state estimate would be propagated forward to real-time from the latest completed smoothing window. Superior orbit estimate accuracy will derive from use of GPS carrier-phase measurements and estimation of carrier-phase range biases.

Development Status

An effort is currently underway to develop a simulation to validate the concept presented.

DESIRED PROPERTIES

Let A denote the class of *linear* optimal sequential estimators presented by Meditch[6] with members

- Kalman filter (KF)
- fixed-interval smoother
- Carlton-Rauch fixed-epoch smoother
- Frazer fixed-epoch smoother
- fixed-lag smoother
- combination of above

Let $\tilde{A}$ denote the class of *nonlinear* optimal sequential estimators that derive from the linear estimators of class A by extension. And let $\breve{A}$ denote the union of classes A and $\tilde{A}$. For prototype in Class $\tilde{A}$ we have the well-known extended Kalman filter (EKF). Epoch for the KF and EKF is defined by the time-tag t_k of last measurement processed, or by propagation to $t_{k+1} > t_k$. But the epoch for each smoothed state estimate of interest lags the time-tag t_k of last measurement processed by the KF. The state estimate error magnitude is always smallest, thus accuracy is best, at estimation epoch[5] for each member of Class $\breve{A}$. But each smoothed state estimate has better accuracy than a filtered state estimate, at the same epoch, when the smoothed state estimate epoch lags KF measurement time-tags with a significant time-lag. Here the smoother has processed more measurements than the filter, and the smoother estimate derives from information forward of the smoother epoch, and from information prior to the smoother epoch, whereas the filter estimate derives only from information prior to the same epoch. The latter has special significance.

[5] In contrast, note that state estimate error magnitude for each iterative batch least squares (LS) estimate depends on LS data fit span and distribution of data in the fit span. Thus LS state estimate error magnitude is independent of epoch placement.

There exists a class of nonlinear estimation problems that cannot be solved with a real-time extended Kalman filter (EKF) because all tracking data precedes the EKF state epoch, and tracking data following the real-time state epoch are not available. An example is provided by the problem of estimating the velocity change due to an impulsive maneuver at the time of maneuver impulse. The most accurate state estimate must use tracking data both before and after the time of maneuver impulse. A second example is provided by the optimal simultaneous estimation of orbit and atmospheric density with a sequential estimator where use is made of tracking data before the state epoch and tracking data after the state epoch. A third example is provided by the optimal GPS orbit determination and time-transfer problem using GPS pseudo-range measurements and GPS carrier-phase measurements, where carrier-phase range-biases must be estimated at fixed epochs. These examples demonstrate the need for a smoothing lag that is time-variable. Sequential smoothers are useful in solving this class of problems.

ODTK uses an EKF that runs forward with time followed by an extended FIS that runs backward with time. But this filter-smoother of Class $\tilde{A}$ cannot be conveniently used for *near-real-time* estimation because all measurements of interest across the fixed-interval must be completely filtered and smoothed before a smoothed state estimate is available for use. We appear to need a smoother from Class $\tilde{A}$ that runs forward with time to achieve near-real-time orbit determination. Thus we desire an estimator with properties

1. Class $\tilde{A}$
2. runs forward with time (pause acceptable)
3. near-real-time throughput
4. accuracy performance due to optimal smoothing
5. smoothing lag is time-variable

PROPERTIES AVAILABLE

Linear

We have studied smoothers of Class A for extension to Class $\tilde{A}$. Choices are best understood by reviewing particular aspects of Class A estimators for discrete linear systems. The best presentation of Class A estimators was given by Meditch[6], unified theoretically by use of Sherman's Theorem[13][14][6][21], and unified notationally with adoption of Kalman's indexing[1][6]. We choose *discrete* linear systems in preference to *continuous* linear systems because the trajectory measurements for orbit determination of space objects are always discrete. We refer to these linear algorithms with acronyms identified by Table 2. These algorithms have properties summarized in Table 3, where FE refers to the fixed epoch of a fixed epoch smoother.

Class A	Acronym
Kalman Filter	**KF**
Fixed Interval Smoother	**FIS**
Fixed Epoch Smoother/Carlton-Rauch	**FES/CR**
Fixed Epoch Smoother/Frazer	**FES/F**
Fixed Lag Smoother	**FLS**

Table 2: Acronyms for Linear Sequential Estimators

Extension

State estimates of Class A are always propagated with a linear transition matrix function Φ. It is important to note that extension from Class A to Class $\tilde{A}$ can be achieved with two very different techniques. First, propagate *variations* of the state estimate with a linear transition matrix function Φ. It appears that this can always be achieved. Or second, propagate the state estimate directly with a nonlinear transition function φ. It appears that this cannot always be achieved with sequential smoothers.

Class A	**KF**	**FIS**	**FES/CR**	**FES/F**	**FLS**
Initial Conditions	user	terminal KF	KF at FE	KF at FE	after KF-FIS
Time Direction	forward	backward	forward	forward	forward
Throughput	real-time	after KF-FIS	near-real-time	near-real-time	near-real-time
Matrix Inverses	0	1	1	0	3
Extension $\boldsymbol{\varphi}$	yes	yes	no	no	no
Extension Φ	yes	yes	yes	yes	yes

Table 3: Available Properties of Linear Estimators

Nonlinear

Extension $\boldsymbol{\varphi}$ of Table 3 refers to an acceptable conversion of every linear propagation of state estimate to nonlinear numerical integration, for extension from Class A to Class $\tilde{A}$. We have successfully used numerical integration $\boldsymbol{\varphi}$ for extension of KF and FIS algorithms for many years. But this does not appear to be possible for FES/CR, FES/F and FLS algorithms.

Extension Φ of Table 3 refers to the acceptable use of a linear transition matrix function to propagate state estimate *variations*, rather than state estimates, for extension from Class A to Class $\tilde{A}$. The FES/CR algorithm is our first successful example. The EKF measurement residual is a linear variation used successfully without propagation in the EKF. The EKF measurement residual has been successfully propagated linearly in the FES/F algorithm.

The FLS algorithm is rejected for use in our VLS because it does not satisfy Property 5: *smoothing lag is time-variable*. Also, the FLS algorithm is undesireable because it requires the calculation of three state-sized matrix inverses. The FES/F is attractive for use in our VLS because no state-sized matrix inverse is required.

KALMAN FILTER

Time Update

Linear

The Kalman filter linear algorithm is derived and presented by Meditch[6] in Theorem 5.5 page 176. Let t_k be the time of last measurement. We are given the

- $n \times 1$ matrix state estimate $\hat{X}_{k|k}$
- $n \times n$ matrix state estimate error covariance matrix $P_{k|k}$
- $n \times p$ disturbance transition matrix $\Gamma_{k+1,k}$
- $p \times p$ process noise covariance matrix Q_k
- new measurement y_{k+1} at time $t_{k+1} > t_k$

Calculate the propagated state estimate $\hat{X}_{k+1|k}$ and covariance $P_{k+1|k}$

$$\hat{X}_{k+1|k} = \Phi_{k+1,k}\hat{X}_{k|k} \tag{1}$$

$$P_{k+1|k} = \Phi_{k+1,k}P_{k|k}\Phi_{k+1,k}^T + \Gamma_{k+1,k}Q_k\Gamma_{k+1,k}^T \tag{2}$$

Nonlinear

Here we present our particular form for an extended Kalman filter (EKF) Time Update. State estimate propagation is nonlinear, so the linear propagation $\Phi_{k+1,k}\hat{X}_{k|k}$ of Equation 1 must be replaced with a numerical integrator $\varphi\{\cdot\}$

$$\hat{X}_{k+1|k} = \varphi\left\{t_{k+1}; \hat{X}_{k|k}, t_k, u\left(\hat{X}\left(\tau|t_k\right), \tau\right), t_{k+1} \leq \tau \leq t_k\right\} \tag{3}$$

and the propagation $\Gamma_{k+1,k}Q_k\Gamma_{k+1,k}^T$ of white noise covariance Q_k must be replaced with a physically connected non-white noise covariance $P_{k+1,k}^{\int\int}$

$$P_{k+1|k} = \Phi_{k+1,k}P_{k|k}\Phi_{k+1,k}^T + P_{k+1,k}^{\int\int} \tag{4}$$

where $P_{k+1,k}^{\int\int}$ is composed of a sum of doubly integrated acceleration error covariance functions due to gravity, air-drag, solar pressure, and thrusting.

Measurement Update

Linear

Let t_k be the time of last measurement y_k. Given a new scalar measurement y_{k+1} at time $t_{k+1} > t_k$, its non-zero measurement error covariance R_{k+1}, the propagated state estimate $\hat{X}_{k+1|k}$, and the propagated state estimate error covariance matrix $P_{k+1|k}$, and the measurement-state $1 \times n$ row matrix H_{k+1}, calculate

$$\Delta y_{k+1|k} = y_{k+1} - H_{k+1}\hat{X}_{k+1|k} \tag{5}$$

$$\tilde{R}_{k+1} = H_{k+1}P_{k+1|k}H_{k+1}^T + R_{k+1} \tag{6}$$

$$K_{k+1} = P_{k+1|k}H_{k+1}^T\tilde{R}_{k+1|k}^{-1} \tag{7}$$

$$\hat{X}_{k+1|k+1} = \hat{X}_{k+1|k} + K_{k+1}\Delta y_{k+1|k} \tag{8}$$

$$P_{k+1|k+1} = \left(I - K_{k+1}H_{k+1}\right)P_{k+1|k} \tag{9}$$

Nonlinear

Class $\tilde{A}$ is distinguished with the nonlinear measurement representation $y\left(\hat{X}_{k+1|k}\right)$ and calculations

$$H_{k+1} = \left[\frac{\partial y\left(X\right)}{\partial X}\right]_{\hat{X}_{k+1|k}} \tag{10}$$

$$\Delta y_{k+1|k} = y_{k+1} - y\left(\hat{X}_{k+1|k}\right) \tag{11}$$

But calculations for $\tilde{R}_{k+1}$, K_{k+1}, $\hat{X}_{k+1|k+1}$, and $P_{k+1|k+1}$ have the same form as for Class A

$$\tilde{R}_{k+1} = H_{k+1}P_{k+1|k}H_{k+1}^T + R_{k+1} \tag{12}$$

$$K_{k+1} = P_{k+1|k} H_{k+1}^T \tilde{R}_{k+1|k}^{-1} \tag{13}$$

$$\hat{X}_{k+1|k+1} = \hat{X}_{k+1|k} + K_{k+1} \Delta y_{k+1|k} \tag{14}$$

$$P_{k+1|k+1} = \left(I - K_{k+1} H_{k+1}\right) P_{k+1|k} \tag{15}$$

Our ODTK EKF design has been successfully applied to many orbit determination problems. References [18], [19], [24], [25], and [26] exemplify what we mean by physically connected state estimate error covariance function. When processing GPS pseudo-range and carrier phase measurements, an intimate understanding and use of the stochastic GPS composite clock is required, as demonstrated in References [22] and [23]. In summary, our definition of EKF is uniquely specialized by the stochastic physics encountered in the orbit determination problem.

CARLTON-RAUCH FIXED-EPOCH SMOOTHER

FES Initialization

Let t_{FE} denote a fixed epoch, coincident with time centroid of an impulsive spacecraft maneuver and known a priori. Let $\hat{X}_{\mathrm{FE}}$ and P_{FE} denote filtered state estimate and covariance at t_{FE}. Meditch's presentation of the Carlton-Rauch FES denotes t_{FE} as coincident with time-tag of some measurement processed; i.e., $t_{\mathrm{FE}} = t_k$ for $\hat{X}_{\mathrm{FE}} = \hat{X}_{k|k}$ and $P_{\mathrm{FE}} = P_{k|k}$, but this is not necessary[6]. It may be necessary that $\hat{X}_{\mathrm{FE}} = \hat{X}_{k|k-1}$ and $P_{\mathrm{FE}} = P_{k|k-1}$ for propagated state estimate $\hat{X}_{k|k-1}$ and covariance $P_{k|k-1}$. However, to be consistent with Meditch's presentation I shall continue with his notation.

Let $\hat{X}_{k|j-1}$ denote an FES state estimate with fixed epoch t_k where $j = k + 1$, where the last measurement processed by the filter has time-tag t_k or t_{k-1}, and where $t_k \leq t_{j-1}$ or $t_{k-1} \leq t_{j-1}$ respectively. With the filter at time $t_{\mathrm{FE}} = t_k$, initialize the FES by storing objects associated with, or calculated by, the filter. Store t_k and

$$\hat{X}_{k|j-1} = \hat{X}_{\mathrm{FE}} \tag{16}$$

$$P_{k|j-1} = P_{\mathrm{FE}} \tag{17}$$

$$\hat{X}_{j-1|j-1} = \hat{X}_{\mathrm{FE}} \tag{18}$$

$$P_{j-1|j-1} = P_{\mathrm{FE}} \tag{19}$$

$$B_{j-1} = I \tag{20}$$

Measurement at $t_j = t_{k+1}$

For this section $j = k+1$, where t_k is the fixed epoch and $t_j > t_k$ is the time-tag for a new measurement $y_j = y_{k+1}$.

[6] If one processes a pseudo-measurement with time-tag t_{FE} that has zero measurement-state partial derivatives, then Meditch's notation is maintained and no harm is done to the VLS.

Filter

The filter calculates the propagated state estimate $\hat{X}_{k+1|k} = \hat{X}_{j|j-1}$, propagated covariance $P_{k+1|k} = P_{j|j-1}$, filtered state estimate $\hat{X}_{k+1|k+1} = \hat{X}_{j|j}$, filtered covariance $P_{k+1|k+1} = P_{j|j}$, and transition matrix $\Phi_{k+1,k} = \Phi_{j,j-1}$. Store $\hat{X}_{j|j-1}$, $P_{j|j-1}$, $\hat{X}_{j|j}$, $P_{j|j}$, and $\Phi_{j,j-1}$ for use in the FES. For the first value of B_j, following FES initialization, set

$$B_j = B_{j-1} A_{j-1} \tag{21}$$

where

$$A_{j-1} = P_{j-1|j-1} \Phi_{j,j-1}^T P_{j|j-1}^{-1} \tag{22}$$

FES

FES calculations refer to the fixed epoch t_k, and to filter measurement time-tags $t_j \geq t_k$.

$$\hat{X}_{k|j} = \hat{X}_{k|j-1} + B_j \left[\hat{X}_{j|j} - \hat{X}_{j|j-1} \right] \tag{23}$$

$$P_{k|j} = P_{k|j-1} + B_j \left[P_{j|j} - P_{j|j-1} \right] B_j^T \tag{24}$$

If the column matrix $\hat{X}_{k|j}$ has n elements, then $P_{k|j}$, $P_{k|j-1}$, $P_{j|j-1}$, $P_{j|j}$, B_j, and $\Phi_{j,j-1}^T$ are $n \times n$ matrices. Covariance matrices $P_{k|j}$, $P_{k|j-1}$, $P_{j|j-1}$, and $P_{j|j}$ are symmetric and are free of negative eigenvalues. Zero eigenvalues in $P_{j|j-1}$ are not acceptable because it must be inverted. The implementation must guarantee that symmetric matrices are numerically symmetric, that all covariance matrices are numerically free of negative eigenvalues, and that $P_{j|j-1}$ is free of zero eigenvalues.

Filter

After FES execution and recording of FES results, the FES recursion is performed by the filter in preparation for the next measurement.

$$\hat{X}_{k|j-1} = \hat{X}_{k|j} \tag{25}$$

$$P_{k|j-1} = P_{k|j} \tag{26}$$

$$B_{j-1} = B_j \tag{27}$$

Measurements at $t_j = t_{k+1},\ t_{k+2}, \ldots$

In the section *Measurement at* $t_j = t_{k+1}$ above, replace t_{k+1} with t_{k+2} for the measurement $y_j = y_{k+2}$ at time $t_j = t_{k+2}$. When $t_j = t_{k+h}$, replace t_{k+1} with t_{k+h} for the measurement $y_j = y_{k+h}$ at time $t_j = t_{k+h}$.

FRAZER FIXED-EPOCH SMOOTHER

FES Initialization

Let t_{FE} denote a fixed epoch, coincident with time centroid of an impulsive spacecraft maneuver and known a priori. Let $\hat{X}_{\text{FE}}$ and $\hat{P}_{\text{FE}}$ denote filtered state estimate and covariance at t_{FE}. Meditch's presentation ([6] Corollary 6.1 page 232) of the Frazer FES denotes t_{FE} as coincident with time-tag of some measurement processed; i.e., $t_{\text{FE}} = t_k$ for $\hat{X}_{\text{FE}} = \hat{X}_{k|k}$ and $P_{\text{FE}} = P_{k|k}$, but this is not necessary[7]. It may be necessary that $\hat{X}_{\mathrm{FE}} = \hat{X}_{k|k-1}$ and $P_{\mathrm{FE}} = P_{k|k-1}$ for propagated state estimate $\hat{X}_{k|k-1}$ and covariance $P_{k|k-1}$. However, to be consistent with Meditch's presentation I shall continue with his notation.

Let $\hat{X}_{k|j-1}$ denote an FES state estimate with fixed epoch t_k where $j = k+1$, where the last measurement processed by the filter has time-tag t_k or t_{k-1}, and where $t_k \le t_{j-1}$ or $t_{k-1} \le t_{j-1}$ respectively. With the filter at time $t_{\mathrm{FE}} = t_k$, initialize the FES by storing objects associated with, or calculated by, the filter: t_k, $\hat{X}_{k|j-1} = \hat{X}_{\mathrm{FE}}$, $P_{k|j-1} = P_{\mathrm{FE}}$, and $W_{j-1} = P_{\mathrm{FE}}$.

Measurement at $t_j = t_{k+1}$

For this section $j = k+1$, where t_k is the fixed epoch and $t_j > t_k$ is the time-tag for a new measurement $y_j = y_{k+1}$.

Filter

The filter calculates the propagated state estimate $\hat{X}_{k+1|k} = \hat{X}_{j|j-1}$, propagated covariance $P_{k+1|k} = P_{j|j-1}$, filtered state estimate $\hat{X}_{k+1|k+1} = \hat{X}_{j|j}$, filtered covariance $P_{k+1|k+1} = P_{j|j}$, transition matrix $\Phi_{k+1,k} = \Phi_{j,j-1}$, measurement-state jacobian matrix $H_{k+1} = H_j$, measurement covariance matrix $R_{k+1} = R_j$, and measurement residual $\Delta y_{k+1,k} = \Delta y_{j,j-1}$ at time-tag $t_{k+1} = t_j$ for the new measurement $y_{k+1} = y_j$. Store $\hat{X}_{j|j-1}$, $P_{j|j-1}$, $X_{j|j}$, $P_{j|j}$, $\Phi_{j,j-1}$, H_j, R_j, and $\Delta y_{j,j-1}$ for use in the FES.

FES

The following algorithm was constructed by Frazer ([6] Corollary 6.1 page 232). Fixed epoch smoother calculations refer to the fixed epoch t_k, and to filter measurement time-tags $t_j \ge t_k$.

$$S_j = H_j^T R_j^{-1} H_j \tag{28}$$

$$W_j = W_{j-1} \Phi_{j,j-1}^T \left[I - S_j P_{j|j} \right] \tag{29}$$

$$\hat{X}_{k|j} = \hat{X}_{k|j-1} + W_j H_j^T R_j^{-1} \Delta y_{j,j-1} \tag{30}$$

$$P_{k|j} = P_{k|j-1} - W_j \left[S_j P_{j|j-1} S_j + S_j \right] W_j^T \tag{31}$$

If the column matrix $\hat{X}_{k|j}$ has n elements, then $P_{k|j}$, $P_{k|j-1}$, $P_{j|j-1}$, $P_{j|j}$, $\Phi_{j,j-1}^T$, S_j, and W_j are $n \times n$ matrices. Covariance matrices $P_{k|j}$, $P_{k|j-1}$, $P_{j|j-1}$, and $P_{j|j}$ are symmetric matrices with positive or zero eigenvalues. Zero covariance matrix eigenvalues are acceptable because no state-sized covariance matrix inverse is required for Frazer form of the FES. S_j is seen to be symmetric by inspection of it's defining Equation 28. The implementation must guarantee that symmetric matrices are numerically symmetric, and that covariance matrices are numerically free of negative eigenvalues. W_{j-1} is initialized as a symmetric covariance matrix, but W_j and subsequent W_{j-1} matrices are not symmetric due to the factor $\Phi_{j,j-1}^T$ in the recursive Equation 29.

FES calculations require products of matrices with extreme differences in order of magnitude. For example, the calculation of W_j according to Equation 29 requires evaluation of the product $S_j P_{j|j}$ that is subtracted from a matrix of order unity. The eigenvalues of S_j are very large due to the small values of R_j, and the eigenvalues of $P_{j|j}$ are very small, all non-negative. The product $S_j P_{j|j}$ is of order unity, but some significance is lost in double precision calculations. It may thus be advisable to premultiply S_j by a small positive scalar ϵ and premultiply $P_{j|j}$ by it's inverse ϵ^{-1} for calculation of the product $S_j P_{j|j} = (S_j \epsilon) \left(\epsilon^{-1} P_{j|j} \right)$, where $(S_j \epsilon)$ and $\left(\epsilon^{-1} P_{j|j} \right)$ are both of order unity.

[7] If one processes a pseudo-measurement with time-tag t_{FE} that has zero measurement-state partial derivatives, then Meditch's notation is maintained and no harm is done to the VLS.

Filter

After FES execution and recording of FES results, the FES recursion is performed by the filter in preparation for the next measurement.

$$\hat{X}_{k|j-1} = \hat{X}_{k|j} \tag{32}$$

$$P_{k|j-1} = P_{k|j} \tag{33}$$

$$W_{j-1} = W_j \tag{34}$$

Measurements at $t_j = t_{k+1},\ t_{k+2}, \ldots$

In the section *Measurement at* $t_j = t_{k+1}$ above, replace t_{k+1} with t_{k+2} for the measurement $y_j = y_{k+2}$ at time $t_j = t_{k+2}$. When $t_j = t_{k+h}$, replace t_{k+1} with t_{k+h} for the measurement $y_j = y_{k+h}$ at time $t_j = t_{k+h}$.

References

[1] Kalman, R. E., *New Methods in Wiener Filtering Theory,* Proceedings of the First Symposium on Engineering Applications of Random Function Theory and Probability, edited by J. L. Bogdanoff and F. Kozin, John Wiley & Sons, New York, 1963

[2] Larson, Kristine, Levine, Judah, *Time Transfer Using the Phase of the GPS Carrier*, IEEE Transactions on Ultrasonics, Ferroelectrics, and Frequency Control, Vol. 46, No. 4, July 1999

[3] Larson, Kristine, Levine, Judah, *Carrier Phase Time Transfer*, IEEE Transactions on Ultrasonics, Ferroelectrics, and Frequency Control, Vol. 47, No. 2, March 2000

[4] Larson, Kristine, Levine, Judah, Nelson, Lisa M., Parker, Thomas E., *Assessment of GPS Carrier-Phase for Time-Transfer Applications*, IEEE Transactions on Ultrasonics, Ferroelectrics, and Frequency Control, Vol. 46, No. 4, July 1999

[5] Larson, Kristine, Private Communication (e-mail), 9 July 2007

[6] Meditch, J. S., *Stochastic Optimal Linear Estimation and Control*, McGraw-Hill, New York, 1969.

[7] Meditch, J. S., *Orthogonal Projection and Discrete Optimal Linear Smoothing*, SIAM J. Control, vol. 5, p. 74, 1967

[8] Meditch, J. S., *A Survey of Data Smoothing for Linear and Nonlinear Dynamic Systems*, Automatica, Vol. 9, pp. 151-162, 1973

[9] Meditch, J. S., Personal Communications, The Aerospace Corporation, 1974.

[10] Parker, Thomas E., Private Communication (Geneva), 30 May 2007

[11] Rauch, H. E., *Solutions to the Linear Smoothing Problem*, IEEE Trans.Autom. Control, vol. AC-8, p. 371, 1963

[12] Rauch, H. E., Tung, F., Striebel, C. T., *Maximum Likelihood Estimates of Linear Dynamical Systems*, AIAA J., vol 3, p. 1445, 1965

[13] Sherman, S., *A Theorem on Convex Sets with Applications*, Ann. Math. Stat., 26, 763-767, 1955.

[14] Sherman, S., *Non-Mean-Square Error Criteria*, IRE Transactions on Information Theory, Vol. IT-4, 1958.

[15] Wright, J. R., *Sequential Orbit Determination with Auto-Correlated Gravity Modeling Errors,* AIAA, Journal of Guidance and Control, Vol 4, No. 2, May-June 1981, page 304.

[16] Wright, J. R., *Orbit Determination Solution to the Non-Markov Gravity Error Problem,* AAS/AIAA Paper AAS 94-176, AAS/AIAA Spaceflight Mechanics Meeting, Cocoa Beach, FLA, Feb., 1994.

[17] Wright, James R., *Optimal Orbit Determination*, Paper AAS 02-192, AAS/AIAA Space Flight Mechanics Meeting, San Antonio, Texas, 27-30 Jan., 2002.

[18] Wright, James R., *Real-Time Estimation of Local Atmospheric Density*, Paper AAS 03-164, 13th AAS/AIAA Space Flight Mechanics Meeting, Ponce, Puerto Rico, 9-13 Feb., 2003

[19] Wright, James R., Woodburn, James, *Simultaneous Real-Time Estimation of Atmospheric Density and Ballistic Coefficient*, Paper AAS 04-175, 14th AAS/AIAA Space Flight Mechanics Conference, Maui, Hawaii, 8-12 Feb., 2004

[20] Wright, James R., Tanygin, Sergei, *Removal of Arbitrary Discontinuities in Atmospheric Density*, Paper AAS 04-176, 14th AAS/AIAA Space Flight Mechanics Conference, Maui, Hawaii, 8-12 Feb., 2004

[21] Wright, James R., *Sherman's Theorem*, The Malcolm D. Shuster Astronautics Symposium, The Journal of the Astronautical Sciences, Vol. 54, Nos. 3 and 4, July - December 2006, pp. 299 - 319

[22] Wright, James R, *Composite Clocks with Three-State Models*, Paper 33, Thirty-Ninth Annual Precise Time and Time Interval (PTTI) Systems and Applications Meeting, Hyatt Regency, Long Beach, CA, November 2007

[23] Wright, James R, *GPS Composite Clock Analysis* (two-state clocks), Hindawi Publishing Corporation, International Journal of Navigation and Observation, Volume 2008, Article ID 261384

[24] Wright, James R, Woodburn, James, Truong, Son, Chuba, William, *Orbit Gravity Error Covariance*, Paper AAS 08-157, 18^{th} AAS/AIAA Space Flight Mechanics Meeting, Galveston, Texas, January 2008

[25] Wright, James R, Woodburn, James, Truong, Son, Chuba, William, *Sample Orbit Covariance Function and Filter-Smoother Consistency Tests*, Paper AAS 08-159, 18^{th} AAS/AIAA Space Flight Mechanics Meeting, Galveston, Texas, January 2008

[26] Wright, James R, Woodburn, James, Truong, Son, Chuba, William, *Orbit Covariance Inner Integrals with Polynomials*, Paper AAS 08-161, 18^{th} AAS/AIAA Space Flight Mechanics Meeting, Galveston, Texas, January 2008

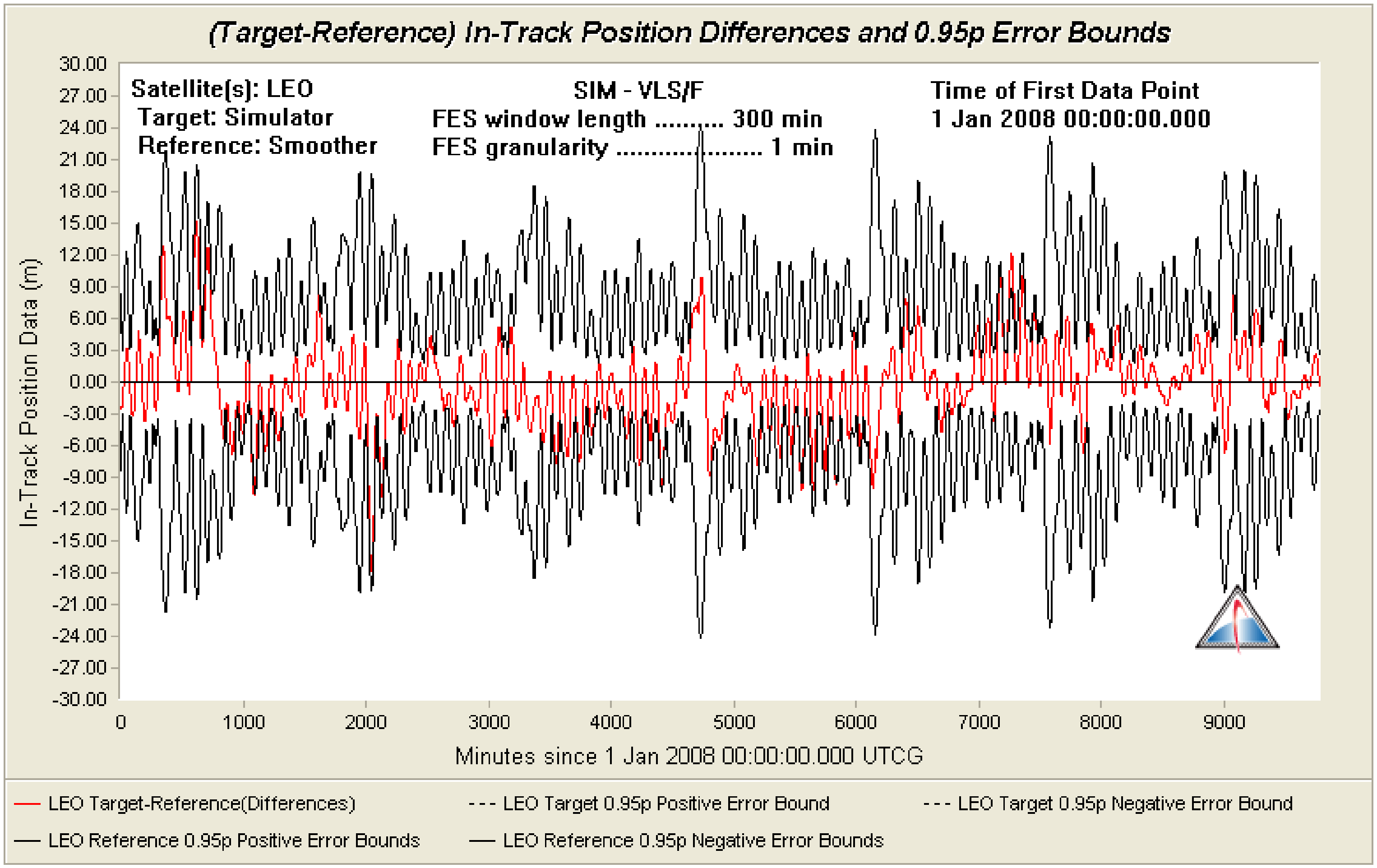

Figure 5: Variable Lag Smoother vs Simulated Truth

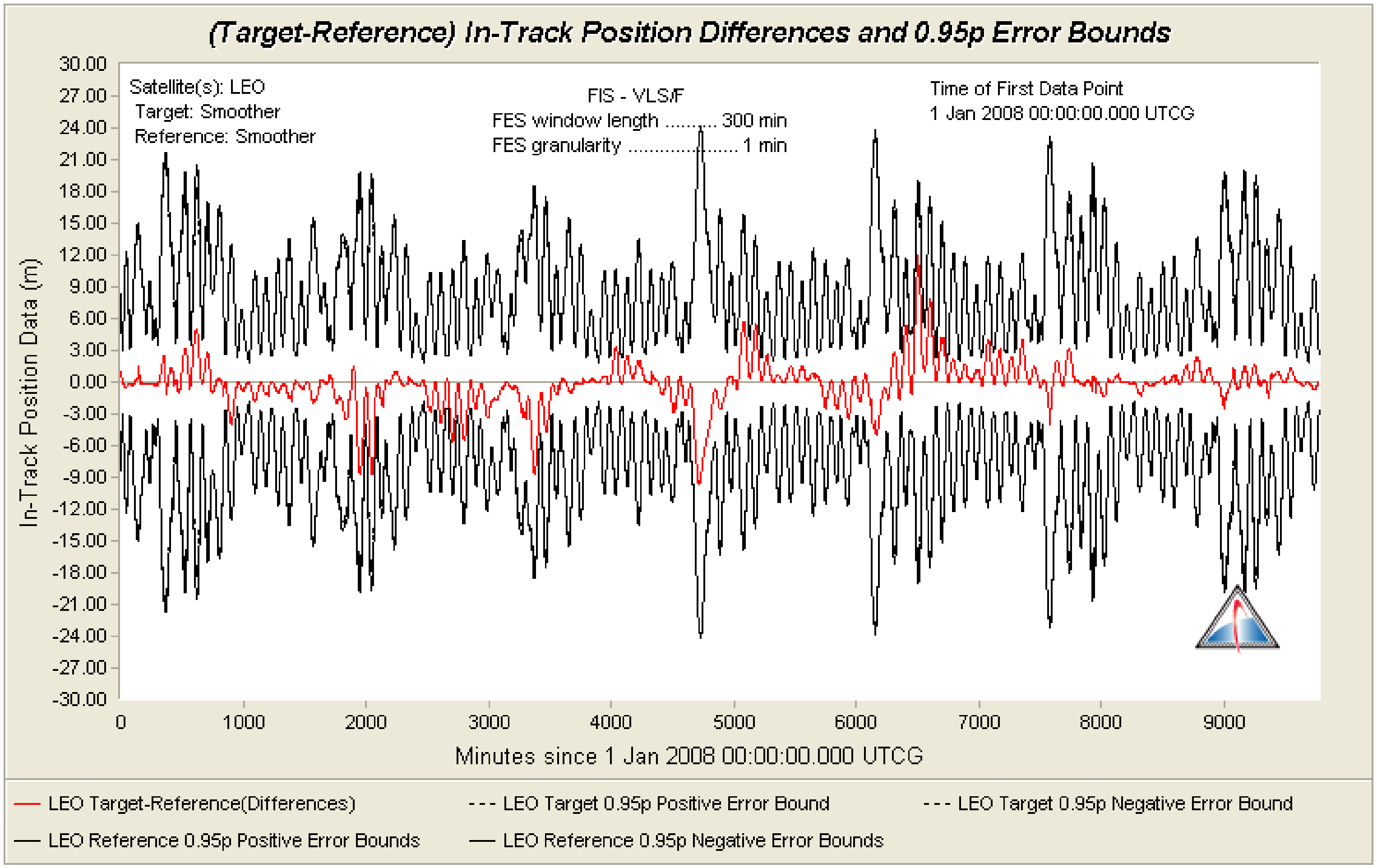

Figure 6: Fixed Interval Smoother vs Variable Lag Smoother

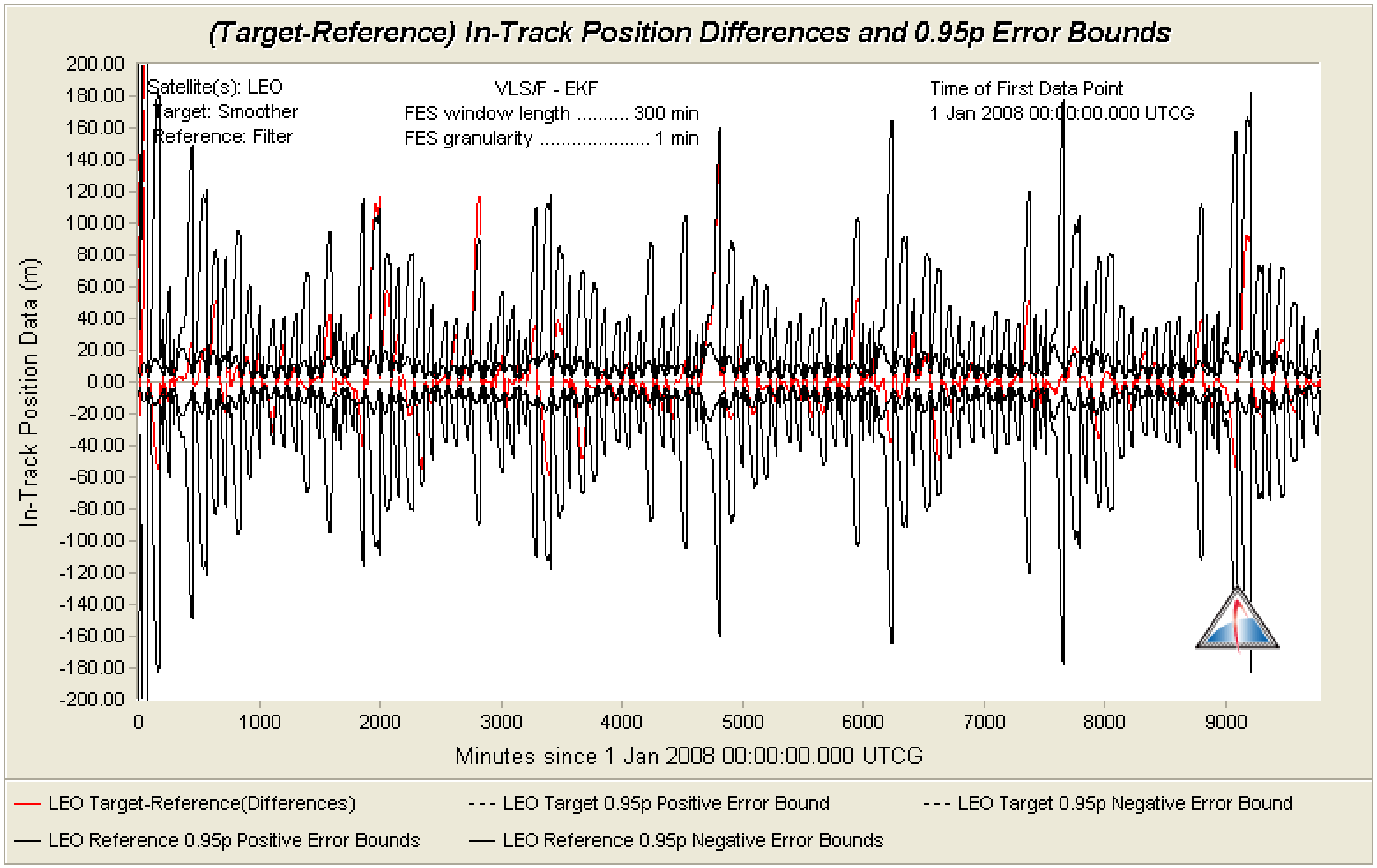

Figure 7: Variable Lag Smoother vs Extended Kalman Filter

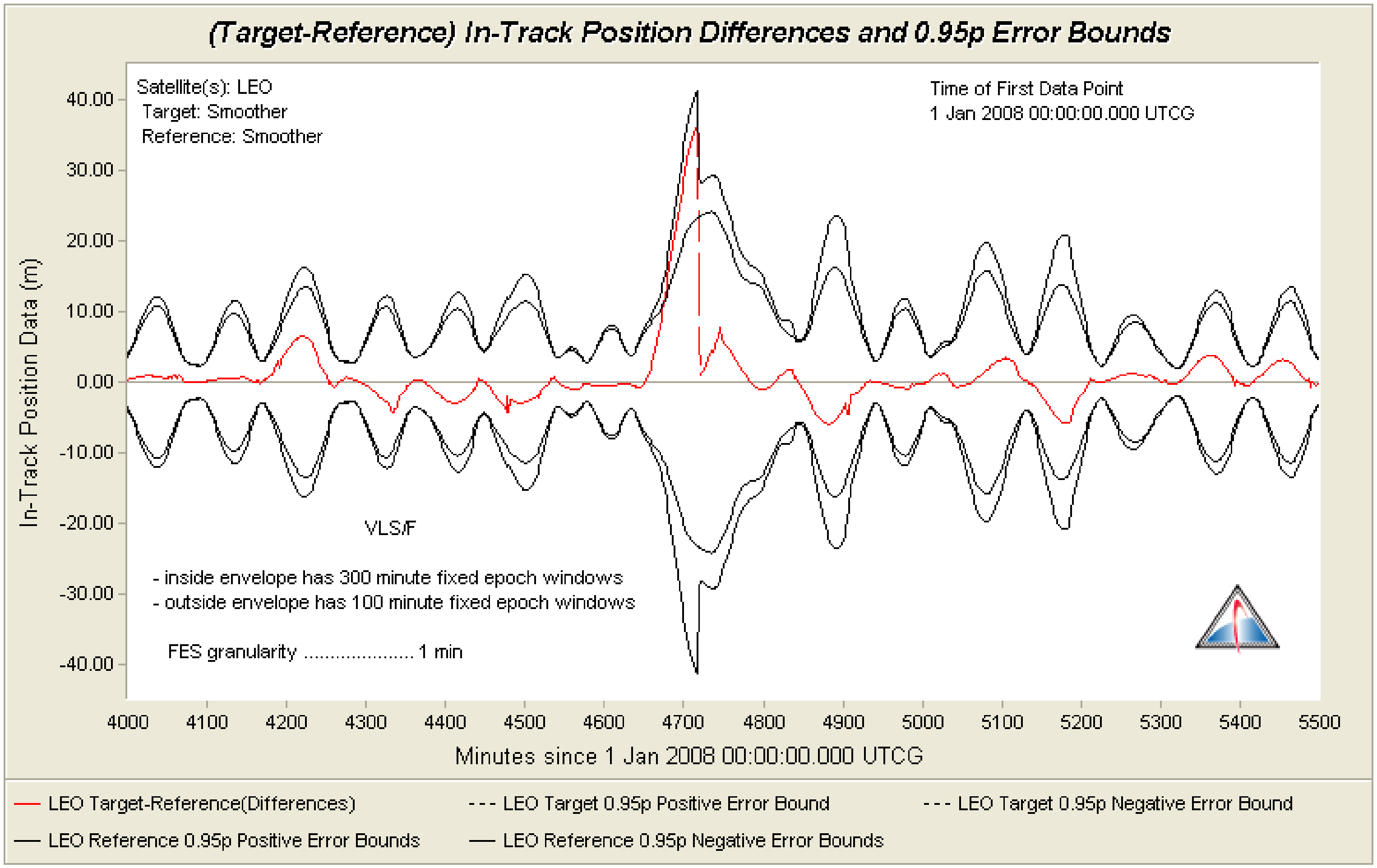

Figure 8: FES Windows: 300 Minutes vs 100 Minutes

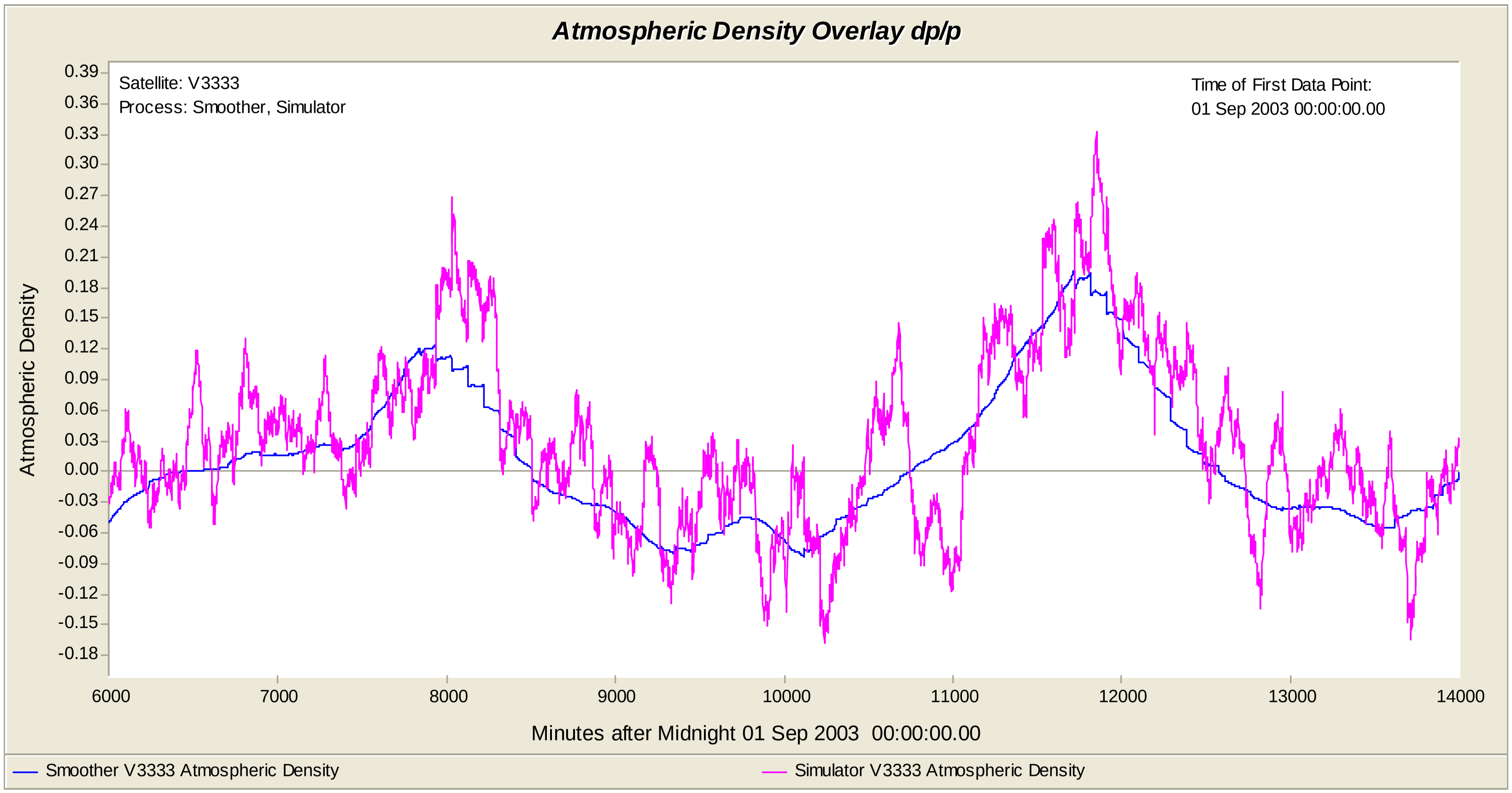

Figure 9: FIS Estimates of Atmospheric Density Ratios

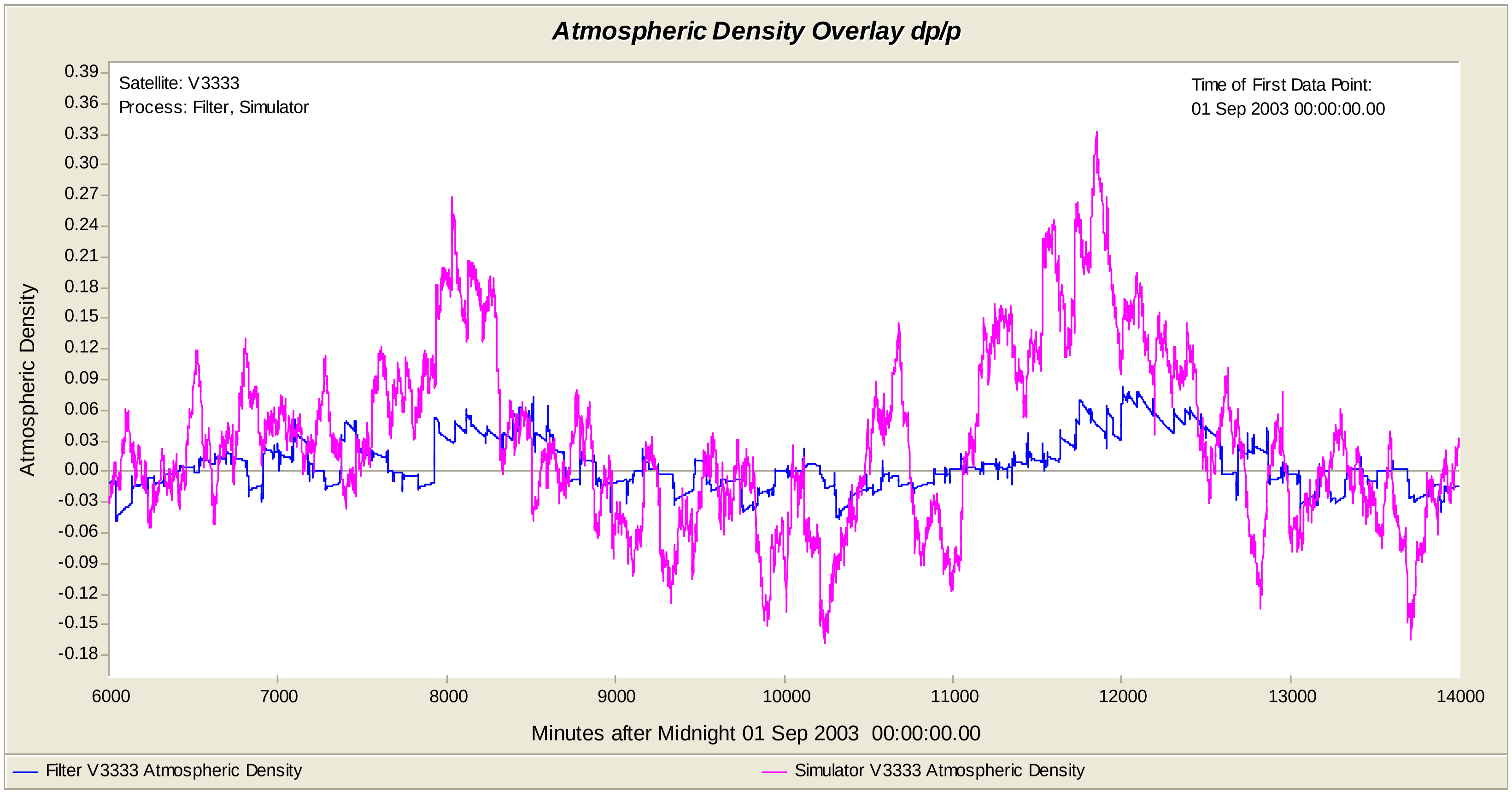

Figure 10: EKF Estimates of Atmospheric Density Ratios